Atmospheric Research 101 (2011) 553–561

Contents lists available at ScienceDirect

Atmospheric Research

journal homepage: www.elsevier.com/locate/atmos

Becker–Döring rate equations for heterogeneous nucleation, with direct vapour deposition and surface diffusion mechanisms

Christiane M. Losert-Valiente Kroon [a,b,*], Ian J. Ford [a,b]

[a] Department of Physics and Astronomy, University College London, Gower Street, London WC1E 6BT, UK
[b] London Centre for Nanotechnology, 17-19 Gordon Street, London WC1H 0AH, UK

ARTICLE INFO

Article history:
Received 7 January 2010
Accepted 12 December 2010

Keywords:
Heterogeneous nucleation
Becker–Döring equations
Fletcher theory

ABSTRACT

We develop a set of microscopic rate equations describing the growth and decay of molecular clusters adsorbed onto a seed particle. Such Becker–Döring equations are fundamental to descriptions of homogeneous nucleation, but do not appear to have been developed for the rather more complicated case of heterogeneous nucleation. We show that the familiar Fletcher theory of heterogeneous nucleation emerges from such a Becker–Döring description, but only if the concentration of adsorbed single molecules on the surface is estimated in a rather rudimentary manner. For small seed particles, this approach fails and one needs a proper Becker–Döring approach to provide a better estimate. The change in predicted nucleation rate can be several orders of magnitude for nanometre-size seed particles. We go on to include into the Becker–Döring treatment the processes of growth and decay of clusters by monomer surface diffusion on the seed. We use recent high quality experimental data to show that the latter process can make only a small contribution to the nucleation current for nanoparticle seeds. We also use the data to demonstrate that the traditional Fletcher theory fails to account for critical sizes and nucleation currents correctly, and that a modification to the implied underlying cluster properties is necessary.

1. Introduction

The theory of heterogeneous nucleation of droplets on suspended seed particles has for many years been neglected in favour of the 'simpler' process, that of homogeneous nucleation in the absence of seeds. One reason is the complication of including a third phase into the system. The crucial surface properties of the seed particles might be difficult to characterise. A second reason is the absence, until recently, of high quality experimental data for the heterogeneous process. A third reason might be a natural reluctance of many in the field to address the more complex heterogeneous nucleation problem before a complete understanding of the homogeneous process is achieved. These reasons perhaps explain why it is hard to find treatments in the literature that go beyond the very rudimentary Fletcher theory of heterogeneous nucleation (and its derivatives). These treatments follow the classical theory of homogeneous nucleation in ignoring the microscopic nature of the seed and the droplet, instead of employing ideas based on continuum physics, scaled down to the nanometre size range. The model is based on the idea of thermodynamic fluctuations that generate a new particle by taking the system over a thermodynamic barrier.

On the other hand, heterogeneous nucleation is a much more typical process in the Earth's atmosphere. Homogeneous nucleation, where seeds are not present, requires vapour pressures that are several times higher than the saturated vapour pressure in order to drive the formation of new droplets. Such conditions of high supersaturation are not normally found in the atmosphere, and virtually never for water, the most common condensable vapour. Instead, water condensation typically takes place on aerosol particles of previously nucleated or mechanically generated organic or inorganic materials. The nucleation requires a vapour pressure only slightly higher than

* Corresponding author. Department of Physics and Astronomy, University College London, Gower Street, London WC1E 6BT, UK. Tel.: +44 20 7679 0604.
E-mail addresses: c.kroon@ucl.ac.uk (C.M. Losert-Valiente Kroon), i.ford@ucl.ac.uk (I.J. Ford).

0169-8095/$ – see front matter © 2011 Elsevier B.V. All rights reserved.
doi:10.1016/j.atmosres.2010.12.019

saturation. Indeed the character of the process as a nucleation phenomenon, in which a thermodynamic barrier is overcome by fluctuation, is often not apparent and the process is sometimes referred to as *activation* at a supersaturation threshold, and considered to be deterministic. Atmospheric clouds, both liquid and ice in phase, form by a process of heterogeneous nucleation on such seeds.

The aim of this paper is twofold. The first is to establish a set of equations describing cluster population dynamics analogous to the familiar Becker–Döring equations of homogeneous nucleation. These equations describe the addition and loss of monomers from clusters as a series of binary reactions. It comes as a surprise to us to find no reference in the literature to such equations. They differ from the usual equations through the need to determine the adsorbed monomer concentration, which in homogeneous kinetics is taken to be a given quantity, at fixed vapour supersaturation. The Becker–Döring equations for heterogeneous nucleation are non-linear instead of linear. However, writing them down is straightforward, and so is their numerical solution. Having established their structure then allows further development, such as attempts to extend them beyond the mean field approximation. The latter is however beyond the scope of the present article.

Instead the second aim of this paper is to develop equations that include both the direct vapour molecule attachment to an adsorbed cluster, and the attachment of a molecule previously adsorbed on the surface. Again, both mechanisms are well-known in principle, and have been alluded to within the Fletcher theory (Vehkamäki, 2006), but we have not found in previous studies a microscopic description based on appropriate Becker–Döring equations.

The models developed in this paper are only a limited advance beyond the simplified Fletcher theory. We can easily write down Becker–Döring equations, but the rate coefficients are unknown in general. We therefore choose to employ the capillarity approximation and the same geometric assumptions inherent in Fletcher theory. This is done largely to investigate how well the Becker–Döring equations perform as a microscopic equivalent of the Fletcher theory. Nevertheless we find two major drawbacks to Fletcher theory: first, that it rests on an assumed adsorbed monomer concentration that seriously underestimates the correct concentration for small seed particles, and secondly that it cannot incorporate surface diffusion in a reasonable way. Noting the first of these drawbacks is perhaps the central point made in this article.

The organisation of this paper is as follows. We first of all review Fletcher theory, and then an equivalent Becker–Döring kinetic treatment, but including only gain and loss of molecules direct from the vapour phase. We expose the central point that the usual Becker–Döring approach employs an assumed monomer concentration, which could be much too high. A so-called *kinetic* and a *dynamical* treatment of the equations demonstrates the difference. We employ the models to describe recent heterogeneous nucleation experiments of *n*-propanol on nanometre size tungsten oxide seed particles. We show that whilst the Fletcher theory does reasonably well in explaining the onset saturations, the predicted critical sizes[1] (corresponding to the size of the cluster that is equally likely to grow or to decay) are very poorly accounted for, as are the nucleation rates. We therefore modify the capillarity approximation to produce a slightly more successful model and note that more detailed microscopic information is needed. Finally, we incorporate the surface diffusion mechanism and show how the dynamical model predictions are affected by this inclusion. For the experimental data under consideration, it turns out that the surface diffusion process does not make a large contribution to the nucleation current, largely because the seeds are so small and there is little room on the surface for more than one adsorbed cluster or monomer.

2. Classical nucleation theory — direct vapour deposition mechanism

2.1. Fletcher theory

In classical heterogeneous nucleation theory a critical cluster is formed on a pre-existing surface (Fletcher, 1958). The seed particle is assumed to be spherical and the critical cluster is assumed to be a cap-shaped part of a sphere — see Fig. 1. The radius of the critical cluster is equal to that of a homogeneous critical cluster under the same conditions (Vehkamäki, 2006). There are several drawbacks to this model, among them is the assumed constant contact angle, that is the angle between the tangents to the solid surface (seed particle) and the liquid surface (cluster), and the constant surface tensions between the contact interfaces. The physical properties of a microscopic entity are assumed to be the same as for a bulk liquid (the capillarity approximation). The assumption of a continuum model of the geometry is a poor approximation especially for small cluster sizes, and

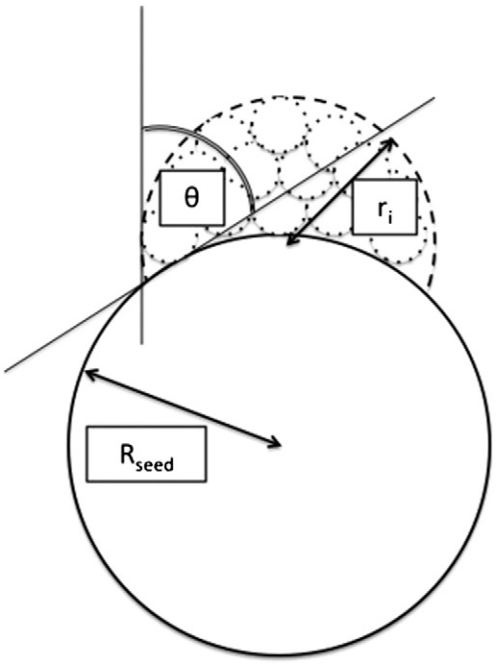

Fig. 1. Illustration of a cluster with radius r_i on the surface of a spherically symmetric seed particle with radius R_{seed} and contact angle θ according to Fletcher theory.

[1] In this context, the term "critical size" refers to the number of molecules building up the cluster and not to the diameter of the cluster.

should be revised. Nevertheless, we can use it to explore the kinetics of heterogeneous nucleation through establishing Becker–Döring rate equations (Becker & Döring, 1935) and (Volmer, 1939).

2.2. Becker–Döring theory with direct vapour deposition mechanism

In Becker–Döring theory for heterogeneous nucleation (Vehkamäki, 2006) we distinguish between two different growth and decay processes. In the direct vapour deposition model gas molecules can attach themselves to an existing cluster on the surface of the seed particle and can be evaporated from the cluster back into the gas phase. In the surface diffusion model clusters grow when monomers that are adsorbed onto the surface of the seed diffuse over the particle surface and eventually collide with the cluster. In the same fashion, monomers can be released from clusters to diffuse on the surface of the seed. The concentrations of clusters of a given size are assumed to evolve according to these processes of gain and loss of monomers from the cluster as chemical reactions without memory. In the first part of this article we concentrate on the direct vapour deposition mechanism. The corresponding Becker–Döring rate equations for the mean concentrations $C_i(t)\ \left[m^{-2}\right]$ of clusters of order i for the direct vapour deposition mechanism read

$$\begin{aligned}\frac{d}{dt}C_1(t) &= j-\lambda C_1(t) + \gamma_2^{dv}C_2(t)-\beta_1^{dv}C_1(t),\\ \frac{d}{dt}C_i(t) &= \beta_{i-1}^{dv}C_{i-1}(t)-\gamma_i^{dv}C_i(t)-\beta_i^{dv}C_i(t) + \gamma_{i+1}^{dv}C_{i+1}(t),\end{aligned} \tag{1}$$

where $\gamma_{i_{max}+1}^{dv}=0$ and the index $i\in[2,\ldots,i_{max}]$. The maximum size of clusters, i_{max}, and hence the maximum number of equations, has to be chosen to be large enough to exceed the order of the critical cluster i^* comfortably. Since growth is more probable than decay for clusters above the critical size, the choice of a cluster sink boundary condition at $i_{max}\gg i^*$ is physically acceptable. Superscripts "dv" indicate processes taking place according to the direct vapour deposition mechanism.

The particular form of the rate coefficients stems from Fletcher theory. The rate coefficient j is called the *source rate* and gives the monomer flux per unit area and per unit time. It takes the form

$$j=\frac{pS}{\sqrt{2\pi mkT}}\left[\frac{1}{sm^2}\right], \tag{2}$$

where p is the pressure $\left(\left[Nm^{-2}\right]\right)$, $S>1$ stands for the vapour phase saturation ratio (dimensionless) defined as the vapour pressure divided by the saturated vapour pressure, m is the molecular mass of a gas molecule ($[kg]$), k the Boltzmann constant $\left(\left[m^2kgs^{-2}K^{-1}\right]\right)$ and T the temperature ($[K]$). The evaporation rate λ characterises the process of evaporation of molecules from the seed surface back into the vapour phase and is given by

$$\lambda=\nu\,exp\left(-\frac{L}{kT}\right)\left[\frac{1}{s}\right], \tag{3}$$

where ν is the adsorbed monomer vibration frequency $\left(\left[s^{-1}\right]\right)$ and L the latent heat of evaporation per monomer ($[Nm]$). The symbol β_i^{dv} denotes the growth rate by the direct vapour deposition mechanism $\left(\left[s^{-1}\right]\right)$ for a cluster of size i, and the symbol γ_{i+1}^{dv} the decay rate by emission of a monomer direct to the vapour $\left(\left[s^{-1}\right]\right)$ for a cluster of size $i+1$. It holds that

$$\beta_i^{dv}<\gamma_i^{dv}\ \text{for}\ i<i^*, \tag{4}$$

$$\beta_i^{dv}\geq\gamma_i^{dv}\ \text{for}\ i\geq i^*, \tag{5}$$

which can be interpreted in the following way: up until the critical cluster size i^* is reached the probability of a cluster to decay is greater than the probability to grow. After the critical cluster size is reached it is more probable for a cluster to grow.

The radius r_i of a cluster of size i is derived from the assumption that the volume of the cap-shaped liquid phase V_{cap} is equal to the total volume of all molecules in the cluster combined,

$$\begin{aligned}V_{cap} :=\ & \frac{\pi}{3}r_i^3\left(2-3cos\Psi(r_i,R_{seed},\theta) + cos^3\Psi(r_i,R_{seed},\theta)\right)\\ & -\frac{\pi}{3}R_{seed}^3\left(2-3cos\Phi(r_i,R_{seed},\theta) + cos^3\Phi(r_i,R_{seed},\theta)\right) = iv,\end{aligned} \tag{6}$$

where v is the volume of a molecule in the liquid phase ($[m^3]$), i the number of molecules in the cluster and R_{seed} is the radius of the seed ($[m]$). The two cosines are defined as

$$\begin{aligned}cos\Psi(r_i,R_{seed},\theta) &:= \frac{R_{seed}cos\theta-r_i}{\sqrt{r_i^2 + R_{seed}^2-2r_iR_{seed}cos\theta}},\\ cos\Phi(r_i,R_{seed},\theta) &:= \frac{R_{seed}-r_icos\theta}{\sqrt{r_i^2 + R_{seed}^2-2r_iR_{seed}cos\theta}}.\end{aligned} \tag{7}$$

We are aware of the error that arises from the *packaging problem*, namely the over-estimation of the volume of the cluster, but in Fletcher theory this is neglected.

We calculate the growth rate in the direct vapour approach in the following way

$$\beta_i^{dv}=jA_i^{(v,l)}\left[\frac{1}{s}\right], \tag{8}$$

where the cap area at the vapour-liquid interface is given by

$$A_i^{(v,l)}=2\pi r_i^2(1-cos\Psi(r_i,R_{seed},\theta))\left[m^2\right]. \tag{9}$$

The loss rate in the direct vapour deposition approach is determined via the expression

$$\gamma_{i+1}^{dv}=\left[\beta_i^{dv}exp\left(\frac{\Delta G_{i+1}-\Delta G_i}{kT}\right)\right]\Big|_{S=1}\ \left[\frac{1}{s}\right], \tag{10}$$

where the formation free energy of a cluster of size i takes the form

$$\Delta G_i=\sigma\left(A_i^{(v,l)}-A_i^{(l,s)}cos\theta\right)-ikT\,ln\,S\,[Nm], \tag{11}$$

with the cap area at the liquid–solid interface

$$A_i^{(l,s)} = 2\pi R_{seed}^2(1-cos\Phi(r_i, R_{seed}, \theta))\left[m^2\right], \quad (12)$$

and σ is the surface tension of the vapour-liquid interface $\left(\left[Nm^{-1}\right]\right)$. We base Eq. (11) on a requirement of detailed balance in the saturated equilibrium between vapour and liquid phase, that is when the saturation ratio is taken to be equal to one.

2.3. Experiment

We will illustrate our theoretical investigations by comparing the calculations in the Fletcher and Becker–Döring frameworks with the experimental data obtained in (Winkler et al., 2008). In the particular experiment, organic vapour, namely n-propanol, condensed on molecular ions as well as on charged and uncharged inorganic nanoparticles, namely tungsten oxide particles. The activation of the pre-existing seed particles was triggered by heterogeneous nucleation. Vapour supersaturation was achieved by adiabatic expansion in a thermostated expansion chamber of a Size Analyzing Nuclei Counter (SANC). Droplet growth was observed by the Contact Angle Mie Scattering detection method (CAMS).

For each vapour saturation ratio S the fraction of activated particles relative to the total number concentration was determined, and used to create a nucleation-activation probability curve depending on the vapour supersaturation ratio for seed diameters ranging from 0.9 nm to 4 nm. The smaller the size of the seed the higher was the vapour supersaturation needed for the activation of the particles. Each nucleation-activation probability curve can be used to extract the corresponding onset saturation ratio, which is the vapour saturation ratio where 50% of particles of a specific size is activated. Accordingly, one can plot the onset saturation ratio as a function of the seed particle mobility diameter and compare the experimental data to the theoretical prediction within the Fletcher framework.

We will concentrate on the data representing the neutral tungsten oxide seed particles. In Table 1 we give the values of the parameters used in the calculations according to the experimental set-up. The small contact angle indicates that the seed particle was totally wettable to the vapour phase — see Fig. 2. It has been claimed (Winkler et al., 2008) that Fletcher theory predicts the observed onset activations for neutral particles exceedingly well — see Table 2. We would like to reconsider this statement in terms of the nucleation current, that is the rate at which critical clusters are formed on the surface of the seed particles.

Table 1
List of values for constants as implied by the experimental set-up (Winkler et al., 2008) and theoretical estimates (Määttänen et al., 2007) and (Seki & Hasegawa, 1983).

Constants in SI units	$R_{seed}=1$ nm	$R_{seed}=2$ nm
θ	5.24e-3	
p	535.96	
$S\|_{P=0.5}$	2.62	1.67
m	1e-25	
k	1.38e-23	
T	275	
ν	8.85e11	
L	8.29e-20	
δ	1e-10	
E	8.29e-21	
σ	0.025	
j	2.87e25	1.83e25
λ	290.57	

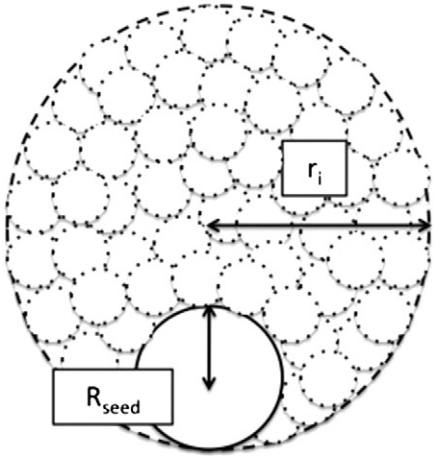

Fig. 2. Illustration of a seed particle with radius R_{seed} totally wettable to the vapour phase, and r_i the radius of the cluster.

This proposed reconsideration is driven by the observation that standard Fletcher theory based on the capillarity approximation leads to disparities between the values of the critical cluster size obtained from theoretical considerations compared to the experimental estimation. The First Heterogeneous Nucleation Theorem (Vehkamäki et al., 2007) together with the nucleation-activation probability curve provides the means to determine the number of molecules in the nucleating cluster. Since the First Heterogeneous Nucleation Theorem is derived from general statistical mechanical considerations this calculation is independent of the model used to describe the cluster. However, one has to be careful concerning the monodispersity of the particles. The number of molecules in the critical cluster as obtained in this fashion will in the sequel be called the *experimental critical cluster size*. In the particular experiment the experimental critical cluster size i^*_{exp} was between twenty and twenty-five. Yet, if one calculates the critical cluster size as predicted by Fletcher theory one finds higher values than the

Table 2
List of calculated quantities: the experimental onset saturation ratio S_{exp}, the onset saturation ratio as obtained from Fletcher theory $S_{Fletcher}$, the experimental critical cluster size i^*_{exp}, the size of the critical cluster as given by Fletcher theory $i^*_{Fletcher}$, the radius of a cluster evaluated for the experimental critical cluster size $r_{i=i^*_{exp}}$, and the radius of a cluster evaluated for the size of the critical cluster as given by Fletcher theory $r_{i=i^*_{Fletcher}}$(equivalent to the Fletcher radius $r^*_{Fletcher}$) for two particular radii of the seed particle R_{seed}.

[SI units]	$R_{seed}=1$ nm	$R_{seed}=2$ nm
S_{exp}	2.62	1.67
$S_{Fletcher}$	2.71	1.87
i^*_{exp}	25	25
$i^*_{Fletcher}$	130	814
$r_{i=i^*_{exp}}$	1.2e-9	2.06e-9
$r_{i=i^*_{Fletcher}}$	1.69e-9	3.17e-9

experimental data imply — see Table 2. This is explored in the next section.

2.4. The heterogeneous nucleation current for the direct vapour deposition mechanism

We want to compare experimental data for the nucleation current with a Fletcher theory of heterogeneous nucleation driven by the direct vapour deposition mechanism, and with the equivalent Becker–Döring model.

2.4.1. Experimental nucleation current

The *experimental nucleation current* (Lazaridis et al., 1992), expressed per unit seed particle surface area and unit time, is given by

$$J_{exp} = -\frac{ln(1-P)}{4\pi R_{seed}^2 t_{exp}}\left[1/\left(m^2 s\right)\right], \tag{13}$$

where R_{seed} is the radius of the seed particle, t_{exp} the activation time and P is the nucleation probability over that time interval. We employ an activation time of $t_{exp}=1$ ms. We take $P=1/2$ and consider J_{exp} to be characterised by the supersaturation S_{exp} corresponding to this condition.

2.4.2. Fletcher nucleation current

The nucleation current as given in Fletcher theory (Fletcher, 1958) reads

$$J_{Fletcher} = K^* exp\left(-\frac{\Delta G^*}{kT}\right), \tag{14}$$

where the symbol ΔG denotes the formation free energy of the critical cluster. The factor K is a kinetic prefactor and is given by

$$K^* = Z^* \beta_{dv}^* C_{ads}, \tag{15}$$

where Z^* is the Zeldovich factor for heterogeneous nucleation processes:

$$Z^* := Z_{hom}^* f(r_{Fletcher}^*, R_{seed}, \theta),$$

$$Z_{hom}^* := \frac{v\sqrt{\sigma}}{2\pi r_{Fletcher}^{*2}\sqrt{kT}},$$

$$f(r_{Fletcher}^*, R_{seed}, \theta) := \sqrt{4}\left(2+\frac{(1-X cos\theta)\left(2-4X cos\theta-\left(cos^2\theta-3\right)X^2\right)}{(1-2X cos\theta+X^2)^{\frac{3}{2}}}\right)^{-\frac{1}{2}} \tag{16}$$

with $X := R_{seed}/r_{Fletcher}^*$. The Fletcher critical cluster radius is given by

$$r_{Fletcher}^* := \frac{2v\sigma}{kT\,ln\,S}. \tag{17}$$

The growth rate of the critical cluster β_{dv}^* in Fletcher theory is

$$\beta_{dv}^* = j 2\pi r_{Fletcher}^{*2}\left(1-cos\Psi\left(r_{Fletcher}^*, R_{seed}, \theta\right)\right). \tag{18}$$

The concentration of the adsorbed monomers is estimated via

$$C_{ads} = \frac{j}{\lambda}. \tag{19}$$

Note that

$$r_{Fletcher}^* = r_{i=i_{Fletcher}^*}, \tag{20}$$

where r_i is determined from Eq. (6) and the heterogeneous critical cluster size in Fletcher theory $i_{Fletcher}^*$ is inserted

$$i_{Fletcher}^* = i_{Fletcher;hom}^* g(r_{Fletcher}^*, R_{seed}, \theta),$$

$$i_{Fletcher;hom}^* := \frac{4\pi r_{Fletcher}^{*3}}{3v},$$

$$g(r_{Fletcher}^*, R_{seed}, \theta) :=$$

$$\frac{1}{4}\left(2+3\frac{1-X cos\theta}{\sqrt{1+X^2-2X\,cos\theta}}-\left(\frac{1-X cos\theta}{\sqrt{1+X^2-2X\,cos\theta}}\right)^3\right)$$

$$-\frac{1}{4}\left(X^3\left(2-3\frac{X-cos\theta}{\sqrt{1+X^2-2X\,cos\theta}}+\left(\frac{X-cos\theta}{\sqrt{1+X^2-2X\,cos\theta}}\right)^3\right)\right). \tag{21}$$

2.4.3. Becker–Döring nucleation currents

Assuming that clusters of order $i_{max}+1$ do not decay, an expression for the nucleation current according to the Becker–Döring equations in the steady state (Becker & Döring, 1935):

$$0 = j-\lambda C_1(t) + \gamma_2^{dv} C_2(t) - \beta_1^{dv} C_1(t),$$

$$0 = \beta_{i-1}^{dv} C_{i-1}(t) - \gamma_i^{dv} C_i(t) - \beta_i^{dv} C_i(t) + \gamma_{i+1}^{dv} C_{i+1}(t),$$

where $\gamma_{i_{max}+1}^{dv}=0$ and the index $i \in [2, \ldots, i_{max}]$, is well known to be

$$J_{BD,kin}\left(C_1^{kin}\right) = \frac{\beta_1^{dv} C_1^{kin}}{1+\sum_{i=2}^{i_{max}}\prod_{j=2}^{i}\frac{\gamma_j}{\beta_j}}, \tag{22}$$

where the mean monomer concentration can again be estimated via

$$C_1^{kin} \approx \frac{j}{\lambda}. \tag{23}$$

We explicitly note that $J_{BD,kin}$ is a function of a specified monomer concentration. The above expression (Eq. 22) may be referred to as the *kinetic Becker–Döring nucleation current*.

The full Becker–Döring equations are in fact non-linear equations for the cluster concentrations, and the steady state solution referred to above is obtained in terms of a given monomer concentration. In a system undergoing heterogeneous nucleation, the monomers are in fact a participating species with a freely variable population. Therefore C_1^{kin} will in general differ from j/λ. To allow for this, we could solve the equations iteratively, using the steady state Becker–Döring solution, or alternatively, simply perform a numerical solution of the time-dependent non-linear differential equations, and identify a steady state solution at late times. The largest cluster size under consideration must satisfy $i_{max} > i^*$, and one therefore has to solve

i_{max} equations for the unknown i-mer concentrations $C_i(t)$. Having done this, we obtain a *dynamical Becker–Döring nucleation current*, defined in simplest form as

$$J_{BD,dyn}(t_\infty) = \beta^{dv}_{i_{max}} C_{i_{max}}(t_\infty), \tag{24}$$

where t_∞ indicates late times corresponding to a steady state solution. Notice that the difference between $J_{BD,dyn}$ and $J_{BD,kin}$ corresponds to the difference between a self-consistent, and an estimated monomer concentration, respectively. One should expect, however, to find that $J_{BD,kin}(C_1(t_\infty)) = J_{BD,dyn}(t_\infty)$.

2.4.4. Comparison of models with data

The Fletcher critical size and onset supersaturation (Eq. 20) are calculated for two particular seed particle sizes in Table 2 and compared with data. The radius of the experimental critical cluster $r_{i=i^*_{exp}}$ is obtained using the experimental critical cluster size i^*_{exp}. The disparity between the model and experimental critical sizes is obvious, even though the onset supersaturations are in reasonable agreement.

Calculations of the nucleation current according to the Fletcher and kinetic Becker–Döring models can be found in Table 3. For a seed radius of value $R_{seed} = 1$ nm we choose the largest cluster size to be $i_{max} = 135$ and for a seed radius of value $R_{seed} = 2$ nm we assume $i_{max} = 820$. We observe that the agreement between the experimental nucleation current J_{exp} and the Fletcher nucleation current $J_{Fletcher}$ is better for a smaller seed radius than for the bigger seed particle. The Fletcher nucleation current $J_{Fletcher}$ and the kinetic Becker–Döring nucleation rate in the steady state $J_{BD,kin}(C_1^{kin})$ are of the same order of magnitude. Clearly, neither is an acceptable description of the data for both seed radii. We shall now attempt to address this by modifying the capillarity approximation.

2.5. The heterogeneous nucleation current for the modified direct vapour deposition mechanism

In order to remove the disparity between the experimental and theoretical critical cluster size we modify parameters such that the critical cluster size as predicted by Fletcher theory, $i^*_{Fletcher}$, coincides with the experimental critical cluster size i^*_{exp}:

$$i^*_{Fletcher} = i^*_{exp} = 25. \tag{25}$$

The simplest way to proceed is to alter the surface tension between the vapour phase and the droplet which we will call the *effective surface tension* σ_{eff} and which is given in Table 4. As a consequence of forcing $i^*_{Fletcher} = i^*_{exp}$ we have $r_{i=i^*_{exp}} = r_{i=i^*_{Fletcher}} = r^*_{Fletcher}$. All other physical and experimental parameters are unchanged. We recalculate the nucleation currents for the various models used in the last subsection with the assumed value $i_{max} = 30$ and summarise the results in Table 5. The Becker–Döring equations are solved with zero initial conditions. Now the modified Fletcher theory overpredicts the nucleation current – compare with Table 3 – yet the result for the bigger seed particle is closer to the experimental nucleation current than in the unmodified theory.

The difference in the values of $J_{BD,kin}(C_1^{kin})$ — see Eq. (22) – and $J_{BD,dyn}(t_\infty)$ — see Eq. (24) – as given in Table 3 arises due to the estimation of the monomer concentration by the ratio j/λ (Eq. 23). This can be illustrated by considering the ratio

$$F(R_{seed}) := \frac{J_{BD,kin}\left(C_1^{kin}\right)}{J_{BD,kin}(C_1(t_\infty))} = \frac{C_1^{kin}}{C_1(t_\infty)}. \tag{26}$$

We have $F(R_{seed} = 1\,\text{nm}) = 1.16\text{e}4$ and $F(R_{seed} = 2\,\text{nm}) = 8.86\text{e}4$. If one recalculates the nucleation rate $J_{BD,kin}$ taking the late time value of the mean monomer concentration $C_1(t_\infty)$ according to the solution of the dynamical Becker–Döring rate equations (Eq. 1) instead of using the estimation for the mean monomer concentration in the steady state (Eq. 23), one finds that

$$J_{BD,kin}[C_1(t_\infty)] = J_{BD,dyn}(t_\infty). \tag{27}$$

as expected. The Fletcher nucleation current $J_{Fletcher}$ clearly overestimates the true nucleation current in the same way as

Table 3
List of the calculated nucleation currents in the various models: the experimental nucleation current J_{exp}, the Fletcher nucleation current $J_{Fletcher}$, and the kinetic Becker–Döring nucleation rate $J_{BD,kin}(C_1^{kin})$ for two particular radii of the seed particle R_{seed}.

Nucleation rate $[m^{-2}s^{-1}]$	$R_{seed} = 1$ nm	$R_{seed} = 2$ nm
J_{exp}	5.52e19	1.38e19
$J_{Fletcher}$	6.32e17	3.61e-8
$J_{BD,kin}(C_1^{kin})$	2.0e18	9.05e-8

Table 4
List of calculated quantities in the modified model: the experimental surface tension σ_{exp}, the effective surface tension σ_{eff}; the experimental critical cluster size i^*_{exp}; the size of the critical cluster as given by Fletcher theory $i^*_{Fletcher}$, the radius of a cluster evaluated for the experimental critical cluster size $r_{i=i^*_{exp}}$, the radius of a cluster evaluated for the order of the critical cluster as given by Fletcher theory $r_{i=i^*_{Fletcher}}$, and the Fletcher radius $r^*_{Fletcher}$ for two particular radii of the seed particle R_{seed}; the experimental onset saturation ratio S_{exp}, and the onset saturation ratio as obtained from Fletcher theory $S_{Fletcher}$.

[SI units]	$R_{seed} = 1$ nm	$R_{seed} = 2$ nm
σ_{exp}	2.51e-2	2.51e-2
σ_{eff}	1.79e-2	1.63e-2
$i^*_{exp} = i^*_{Fletcher}$	25	25
$r_{i=i^*_{exp}} = r_{i=i^*_{Fletcher}} = r^*_{Fletcher}$	1.2e-9	2.06e-9
S_{exp}	2.62	1.67
$S_{Fletcher}$	1.94	1.47

Table 5
List of the calculated nucleation currents in the various modified models: the experimental nucleation current J_{exp}, the Fletcher nucleation current $J_{Fletcher}$, the kinetic Becker–Döring nucleation rate $J_{BD,kin}(C_1^{kin})$, the nucleation rate at late times as derived from the dynamical Becker–Döring rate equations $J_{BD,dyn}(t_\infty)$, and the kinetic Becker–Döring nucleation current obtained with the late time mean monomer concentration as calculated from the dynamical Becker–Döring rate equations $J_{BD,kin}(C_1(t_\infty))$, for two particular radii of the seed particle R_{seed}.

nucleation rate $[m^{-2}s^{-1}]$	$R_{seed} = 1$ nm	$R_{seed} = 2$ nm
J_{exp}	5.52e19	1.38e19
$J_{Fletcher}$	1.79e29	4.81e29
$J_{BD,kin}(C_1^{kin})$	3.32e29	1.62e30
$J_{BD,dyn}(t_\infty)$	2.87e25	1.83e25
$J_{BD,kin}(C_1(t_\infty))$	2.87e25	1.83e25

the kinetic Becker–Döring nucleation rate $J_{BD,kin}$, and for the same reason. Using $J_{BD,dyn}$ the disparity with respect to experimental data is reduced, and the correct tendency for a change in seed radius is obtained.

3. Becker–Döring framework with surface diffusion and direct vapour deposition mechanisms

We continue our investigations incorporating the effective instead of the experimental surface tension. We extend the calculations from the consideration of the direct vapour deposition mechanism only, to the full framework, that is including surface diffusion processes as well as direct vapour deposition processes into our model. The Becker–Döring rate equations for the mean concentrations $C_i(t)\ \left[m^{-2}\right]$ of clusters of order i in the surface diffusion and direct vapour deposition model read

$$\begin{aligned}\frac{d}{dt}C_1(t) &= j-\lambda C_1(t)+\gamma_2^{dv}C_2(t)-\beta_1^{dv}C_1(t)-\beta_1^{sd}C_1(t)\\ &\quad+\gamma_2^{sd}C_2(t)-\sum_{i=1}^{i_{max}}\left(\beta_i^{sd}C_i(t)-\gamma_{i+1}^{sd}C_{i+1}(t)\right),\\ \frac{d}{dt}C_i(t) &= \left(\beta_{i-1}^{dv}+\beta_{i-1}^{sd}\right)C_{i-1}(t)-\left(\gamma_i^{dv}+\gamma_i^{sd}\right)C_i(t)\\ &\quad-\left(\beta_i^{dv}+\beta_i^{sd}\right)C_i(t)+\left(\gamma_{i+1}^{dv}+\gamma_{i+1}^{sd}\right)C_{i+1}(t),\end{aligned} \tag{28}$$

where $\gamma_{i_{max}+1}^{dv}=\gamma_{i_{max}+1}^{sd}\equiv 0$ and the index $i\in[2,\ldots,i_{max}]$. Superscripts "dv" indicate processes taking place according to the direct vapour deposition model, superscripts "sd" denote processes in the surface diffusion model. The rate coefficients $\beta_i^{sd}\left(\left[s^{-1}\right]\right)$ and $\gamma_{i+1}^{sd}\left(\left[s^{-1}\right]\right)$ characterise the surface diffusion processes concerning the growth of a cluster of size i by an adsorbed monomer and the loss of a monomer from a cluster of size $i+1$. The other rate coefficients (j, λ, β_i^{dv}, γ_i^{dv}) are determined as before. The factor of two in the evolution equation for the mean monomer concentration in the surface diffusion terms $\beta_1^{sd}C_1(t)$ and $\gamma_2^{sd}C_2(t)$ arises from the fact that in the surface diffusion mechanism two adsorbed monomers have to collide in order to form a dimer. However, in the direct vapour deposition approach a molecule from the gas phase lands on top of a monomer residing on the surface of the seed, hence the coefficient of unity for the terms $\beta_1^{dv}C_1(t)$ and $\gamma_2^{dv}C_2(t)$. The derivation of the rate coefficients in the surface diffusion model follows that of the rate coefficients in the direct vapour deposition model except that the growth rate coefficient in the surface diffusion model depends on the unknown mean adsorbed monomer concentration, namely

$$\beta_i^{sd}:=\beta_i^{sd}(t)=\beta_i'^{sd}C_1(t)\left[\frac{1}{s}\right], \tag{29}$$

where the constant factor β'^{sd}_i is determined by the number of molecules in a circular region around the cluster, times the vibration frequency leading to jumps, times an exponential function containing the activation energy for surface diffusion, or more precisely,

$$\beta_i'^{sd}=2\pi R_{seed}\delta sin\Phi(r_i,R_{seed},\theta)\nu\ exp\left(-\frac{E}{kT}\right)\left[\frac{m^2}{s}\right], \tag{30}$$

where δ is the average jumping distance ($[m]$), and E the energy of the surface diffusion process ($[Nm]$) (Vehkamäki, 2006). The values of the newly introduced physical parameters used in the following calculations are included in Table 1. The decay rate in the surface diffusion approach can be obtained via

$$\gamma_{i+1}^{sd}=\left[\frac{\beta_i'^{sd}j}{\lambda}exp\left(\frac{\Delta G_{i+1}-\Delta G_i}{kT}\right)\right]\Bigg|_{S=1}\left[\frac{1}{s}\right], \tag{31}$$

which is again derived from a detailed balance argument — see Fig. 3.

Due to the difference of several orders of magnitude between the constant rate coefficients $\beta_i'^{sd}$ and γ_i^{sd} problems in the numerical evaluation of the evolution equations (Eq. 28) arise. In order to avoid these numerical difficulties we employ an estimate of the mean monomer concentration at late times to solve the Becker–Döring rate equations (Eq. 28) iteratively in the following way. The iteration for the mean monomer concentration $C_1(t_\infty)$ at late times t_∞ is performed according to

$$\left[C_1^{m+1}(t_\infty)\right]_{in}=\left(\left[C_1^m(t_\infty)\right]_{out}\left[C_1^m(t_\infty)\right]_{in}\right)^{\frac{1}{2}}, \tag{32}$$

where $\left[C_1^m(t_\infty)\right]_{in}$ is the input value and $\left[C_1^m(t_\infty)\right]_{out}$ the output value in the m-th iteration step. The above estimate for the mean monomer concentration at late times is inserted into the expression for the rate coefficients

$$\beta_i^{sd}=\beta_i'^{sd}\left[C_1^m(t_\infty)\right]_{in} \tag{33}$$

and the system of Becker–Döring rate equations (Eq. 28) is solved. In the zeroth iteration step the mean monomer concentration at late times is estimated to be

$$\left[C_1^0(t_\infty)\right]_{in}=\frac{j}{\lambda}. \tag{34}$$

The iteration procedure is terminated when

$$\frac{\left[C_1^m(t_\infty)\right]_{out}}{\left[C_1^m(t_\infty)\right]_{in}}\approx 1. \tag{35}$$

In our calculation this point is reached when $m=4$ at which $\left[C_1^m(t_\infty)\right]_{out}/\left[C_1^m(t_\infty)\right]_{in}=1\pm O(1e{-}4)$.

The nucleation current from the full Becker–Döring rate equations for both the surface diffusion and the direct vapour deposition mechanisms can be obtained using the expression

$$J_{BD,dyn}(t_\infty)=\left(\beta_{i_{max}}^{dv}+\beta_{i_{max}}'^{sd}C_1(t_\infty)\right)C_{i_{max}}(t_\infty), \tag{36}$$

with $i_{max}>i^*$, where one has to solve i_{max} number of equations. In Table 6 we compare the dynamical Becker–Döring nucleation current as computed for the direct vapour deposition model according to Eq. (24) with the dynamical Becker–Döring nucleation current as computed for both mechanisms according to Eq. (36). One observes that the nucleation current that was calculated taking both the direct vapour deposition and the surface diffusion mechanism into account is generally an order of magnitude less than the nucleation current that results from the consideration of the direct vapour deposition mechanism only. This is a slightly unexpected result but might be rationalised by considering

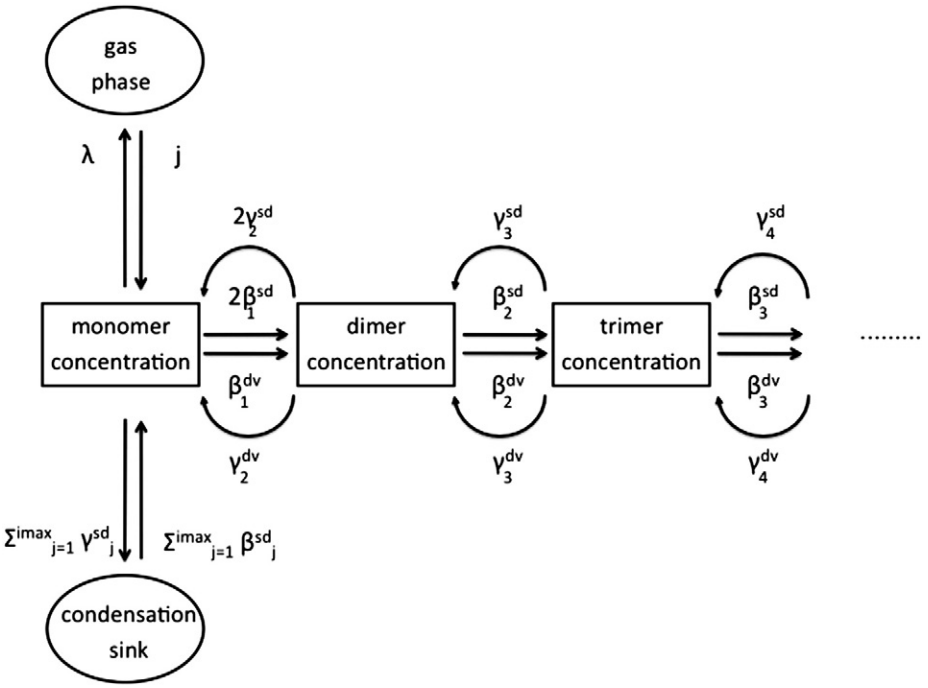

Fig. 3. A schematic of nucleation kinetics according to Becker–Döring theory. Changes in mean *i*-mer concentrations are brought about by the growth of clusters by monomers (β_i) and by the loss of monomers from clusters (γ_i). The superscripts distinguish the direct vapour deposition model from the surface diffusion model. In addition, the mean monomer concentration is altered by an incoming flux of monomers (j) and by the loss of monomers to the gas phase (λ).

that the inclusion of surface diffusion allows both the additional growth, but also additional decay of adsorbed clusters. The additional decay can potentially reduce the nucleation rate since the wider kinetic scheme reduces the concentration of clusters on the surface.

It can be concluded from the relatively small change in the nucleation current that surface diffusion processes do not play an essential role, at least for the heterogeneous nucleation conditions studied in the experiments. A reason for this may be the observation that the linear dimension of a single molecule is of the same order of magnitude as the radius of the seed particle and that very quickly after a heterogeneous nucleus has started to grow, there is little seed surface left for additional adsorbed monomers to diffuse on.

4. Conclusions

In this study we have developed rate equations describing the process of heterogeneous nucleation of droplets on aerosol seed particles. These take the form of the familiar Becker–Döring equations. It is recognised that these are non-linear instead of linear in the cluster populations. Nevertheless the steady state solutions to the equations can be found relatively easily. It appears to us that such a development has not been noted in the literature previously.

The approach demonstrates that the traditional Fletcher theory of heterogeneous nucleation rests on a rather rough estimate of adsorbed monomer concentration, which could be seriously in error for small seed particles. We have developed Becker–Döring models that demonstrate this difference. We have also used the equations to include the additional processes of cluster growth and decay through the surface diffusion mechanism, namely the addition of surface-adsorbed monomers to the cluster, and the reverse. In usual treatments, growth by direct attachment of monomers from the vapour is normally assumed. We show that for nanometre size seed particles, direct attachment makes a dominant contribution to the current, largely because space on the seed particle for additional adsorbed monomers is rather limited. Inclusion of the surface diffusion mechanism reduces the current slightly. For larger seed particles, the inclusion of the surface diffusion mechanism should become more important.

We have studied recent experimental data and concluded that whilst the traditional Fletcher theory might account reasonably well for the onset saturations for heterogeneous nucleation, it fails in detail when considering critical sizes and nucleation currents, particularly with respect to the dependence on seed particle size. We regard Fletcher theory with great caution. It should be recognised that among its many deficiencies it can suffer from an incorrect estimate of adsorbed monomer concentration. Furthermore, like other versions of the classical nucleation theory, Fletcher theory is

Table 6
List of the calculated nucleation currents in the modified models as derived from the dynamical Becker–Döring rate equations in the direct vapour deposition model, $J^{dv}_{BD,dyn}(t_\infty)$, and $J^{sd,dv}_{BD,dyn}(t_\infty)$ as derived from the dynamical Becker–Döring rate equations for the combined mechanism (direct vapour deposition and surface diffusion mechanism) for two particular radii of the seed particle R_{seed}.

Nucleation rate $[m^{-2}s^{-1}]$	$R_{seed}=1$ nm	$R_{seed}=2$ nm
$J^{dv}_{BD,dyn}(t_\infty)$	2.87e25	1.83e25
$J^{sd,dv}_{BD,dyn}((t_\infty)$	1.52e24	1.16e24

founded upon the rather dubious capillarity approximation, as well as inappropriate geometric assumptions for *microscopic* molecular clusters. Analysis of data and estimates of atmospheric behaviour should really be conducted using a truly microscopic theory of heterogeneous nucleation.

Acknowledgements

This work was supported by the Leverhulme Trust under grant F/07134/BV and partly supported by the CN Davies Award of the Aerosol Society.

References

Becker, R., Döring, W., 1935. Kinetische Behandlung der Keimbildung in übersättigten Dämpfen. Ann. Phys. (Leipzig) 24, 719.
Fletcher, N., 1958. Size effect in heterogeneous nucleation. J. Chem. Phys. 29 (3), 572.
Lazaridis, M., Kulmala, M., Gorbunov, B.Z., 1992. Binary heterogeneous nucleation at a non-uniform surface. J. Aerosol Sci. 23 (5), 457.
Määttänen, A., et al., 2007. Two-component heterogeneous nucleation kinetics and an application to Mars. J. Chem. Phys. 127, 134710.
Seki, J., Hasegawa, H., 1983. The heterogeneous condensation of interstellar ice grains. Astrophys. Space Sci. 94 (1), 177.
Vehkamäki, H., 2006. Classical Nucleation Theory in Multicomponent Systems. Springer.
Vehkamäki, H., et al., 2007. Heterogeneous multicomponent nucleation theorems for the analysis of nanoclusters. J. Chem. Phys. 126, 174707.
Volmer, M., 1939. Kinetik der Phasenbildung. Steinkopff, Dresden und Leipzig.
Winkler, P., et al., 2008. Heterogeneous nucleation experiments bridging the scale from molecular ion clusters to nanoparticles. Science 319, 1374.